Atmos. Meas. Tech. Discuss., 3, 2833–2859, 2010
www.atmos-meas-tech-discuss.net/3/2833/2010/
doi:10.5194/amtd-3-2833-2010
© Author(s) 2010. CC Attribution 3.0 License.

Atmospheric Measurement Techniques Discussions

This discussion paper is/has been under review for the journal Atmospheric Measurement Techniques (AMT). Please refer to the corresponding final paper in AMT if available.

Characterization of merged AIRS and MLS water vapor sensitivity through integration of averaging kernels and retrievals

C. K. Liang[1,2], A. Eldering[2], F. W. Irion[2], W. G. Read[2], E. J. Fetzer[2], B. H. Kahn[2], and K.-N. Liou[1]

[1]Joint Institute for Regional Earth System Science and Engineering, Los Angeles, California, USA
[2]Jet Propulsion Laboratory/California Institute of Technology, Pasadena, California, USA

Received: 21 June 2010 – Accepted: 22 June 2010 – Published: 6 July 2010

Correspondence to: C. K. Liang (cliang@atmos.ucla.edu)

Published by Copernicus Publications on behalf of the European Geosciences Union.

Abstract

In this paper, we analyze averaging kernels to assess the sensitivity of the Aqua Atmospheric Infrared Sounder (AIRS) and Aura Microwave Limb Sounder (MLS) to water vapor. The averaging kernels, in the tropical and extra-tropical upper tropospheric and lower stratospheric region of the atmosphere, indicate that AIRS is primarily sensitive to water vapor concentrations typical of tropospheric values up to a level around 260 hPa. At lower pressures AIRS retrievals lose sensitivity to water vapor, though not completely as indicated by the non-zero verticalities at pressures less than 260 hPa. The MLS is able to provide high quality retrievals, with verticalities ∼1 for all pressure levels, down to the same level for where AIRS begins to lose sensitivity. Previous analyses have estimated both instruments to have overlapping sensitivity to water vapor over a half temperature scale height layer, within the upper troposphere, for concentrations between ∼30–400 ppmv. Thus, we implement a method using the averaging kernel information to join the AIRS and MLS profiles into an merged set of water vapor profiles. The final combined profiles are not only smooth functions with height but preserve the atmospheric state as interpreted by both the AIRS and MLS instruments.

1 Introduction

The upper tropospheric/lower stratospheric (UTLS) H_2O budget is largely determined by an interplay between localized convective moistening (Soden, 2004; Horváth and Soden, 2007), dehydration by horizontal advection through precipitating thin cirrus in tropical cold trap regions (Holton and Gettleman, 2001), convective overshoots that mix dry cold dry air into the UTLS region (Sherwood and Dessler, 2001, 2003) and interannual variability events such as the El Niño Southern Oscillation (e.g., Kiladis et al., 2001; Gettelman et al., 2001) and the Quasi-biennial Oscillation (e.g., Reed, 1965a,b; Hamilton, 1984; Dunkerton, 1985).

The radiative impacts of H_2O are substantial in the UTLS. Soden et al. (2007) showed that perturbations to the global distribution of H_2O has the largest radiative impacts on the tropical upper troposphere (UT). Furthermore, the recent drop (mean values between 2001–2005 minus the mean values between 1996–2000) in tropical lower stratospheric (LS) H_2O lead to a radiative forcing of $-0.098\,W/m^2$ which compensated for the $+0.26\,W/m^2$ radiative forcing due to the increase of CO_2 from 1996–2005 (Solomon et al., 2010). Thus, quantifying the UTLS H_2O distribution is crucial to understanding the long-term radiative impacts of H_2O changes due to a warming climate.

Historically, quantification of the UTLS H_2O budget has been hindered by the lack of global high-resolution measurements of H_2O throughout the troposphere and stratosphere. However, recent studies have quantified the global upper tropospheric H_2O structure with the global soundings provided by the "Afternoon Constellation" (A-Train) (Stephens et al., 2002) Atmospheric Infrared Sounder (AIRS) (Aumann et al., 2003) flying on NASA's Aqua satellite platform (Gettelman et al., 2006, 2004; Kahn et al., 2008, 2009). On the same constellation the Microwave Limb Sounder (MLS) (Waters et al., 2006), located on Aura, provides global UTLS H_2O soundings (Read et al., 2007).

The instruments together provide high quality UTLS H_2O measurements, however, AIRS primarily has sensitivity to H_2O consistent with concentrations from the boundary layer up to the UT. The lower threshold of AIRS sensitivity to H_2O was derived empirically, in Gettelman et al. (2004), to be ~10 ppmv based on comparisons with in-situ measurements; Fetzer et al. (2008) found the lower threshold to be between 20–30 ppmv. MLS, however, has sensitivity in the stratosphere down to the UT with sensitivity to values between ~0.1–1 ppmv, but with an upper sensitivity limit of ~500 ppmv (Read et al., 2007). Studies by Read et al. (2007) and Fetzer et al. (2008) attempted to quantify the sensitivity of AIRS and MLS H_2O by direct comparison of retrieved values and found that AIRS and MLS agreed best between ~250–260 hPa.

In this work, however, the newly available AIRS (in the version 5 dataset) and MLS (offline calculation) averaging kernels (AK's) are analyzed to quantify where both in-

struments are most, and least, sensitive to H_2O in the UTLS. Previous work by Maddy and Barnet (2008) computed AIRS AK's for selected sites and approximated the instrument resolution for temperature and H_2O. We use the AK's for an entire year of AIRS retrievals to quantify the instrument's sensitivity to UTLS H_2O. We use this information as a means to merge AIRS and MLS H_2O retrievals into a single profile which spans the troposphere and stratosphere.

2 Data

2.1 Atmospheric profiles

The AIRS version 5 support product (Susskind et al., 2006) and MLS version 2.2 retrievals (Livesey et al., 2006) are co-located for 2008 in the 40 S–40 N latitude band according to Fetzer et al. (2008). Co-location is simply defined as the nearest AIRS footprint to a given MLS footprint (the approximate lag time between Aura to Aqua measurements is about 15 min, but due the MLS viewing geometry the lag is reduced to 8 min). The nearest neighbor co-location is implemented in order to preserve the AIRS resolution. The AIRS reports H_2O mixing ratios as a mean layered quantity between adjacent pressure levels while MLS reports retrievals on a 12 levels per decade change in $\log_{10}P$. Since the MLS reports H_2O as a pressure level quantity, we redefine the AIRS H_2O concentrations as a geometric mean quantity between adjacent pressure levels. These values are then interpolated ($\log(P)$ vs. $\log(H_2O)$) to a hybrid pressure grid that is a combination of the AIRS and MLS grids. The difference in horizontal resolution are not accounted for; the vertical resolution of both instruments are similar (~2–3 km).

Figure 1a is an example of a single AIRS and MLS pair of co-registrated H_2O profiles at 0.17 N and 176 W. When comparing large sets of profiles, one persistent characteristic is that they generally do *not* resemble each other at pressures higher than ~300 hPa; this is well documented in Read et al. (2007) and Fetzer et al. (2008); this is the case

for many other profiles we have analyzed as well. At pressures $100 \leq P \leq 260$ hPa, in the UT (Fig. 1b), the profiles become more similar. However, as seen in Fig. 1b, they do differ enough that a discontinuity exists between the profiles.

One goal of this study is to merge them together in a consistent and rigorous manner in order to form H_2O profiles that span the entire atmospheric column; the "Joined" curve in Fig. 1b is a sample merged profile combining the AIRS (red) and MLS (blue) curves. The merging process is discussed in detail in Sect. 3.2 and requires a quantitative estimate of AIRS and MLS sensitivity to H_2O in the UTLS. This is accomplished with the use of instrument- and retrieval algorithm-specific AK's.

2.2 AIRS averaging kernels

The AIRS AK's are derived on a profile by profile basis at a horizontal spatial resolution of ~45 km; they are computed using the methodology described in Maddy and Barnet (2008). The MLS consists of a single set of AK's for this latitude band. This is because the limb geometry of MLS senses through a large amount of atmosphere, for a given layer, giving it a high sensitivity to H_2O, though with a reduced spatial resolution of about ~200 km along-track. In the case of MLS, the sensitivity is primarily driven by the viewing geometry, so that the AK's do not change much from footprint to footprint. Therefore, herein we focus our analysis on the characterization of the AIRS AK's.

One application of AK's is to degrade high vertical resolution correlative measurements, such as radiosondes of temperature and H_2O for comparison with the more coarsely resolved satellite data (e.g., Maddy and Barnet, 2008). The following equations provide the formalism to do so:

$$\hat{\mathbf{x}} = \hat{\mathbf{x}}_0 + \mathbf{A}(\mathbf{x} - \hat{\mathbf{x}}_0), \tag{1}$$

$$\mathbf{A} = \frac{\partial \hat{\mathbf{x}}}{\partial \mathbf{x}} \tag{2}$$

where the $\hat{\mathbf{x}}$, $\hat{\mathbf{x}}_0$, $\mathbf{A}$, and $\mathbf{x}$ are the smoothed version of the true atmospheric profile, a priori, the AK matrix, and the true atmospheric profile, respectively (Rodgers, 2000).

The AK matrix $\mathbf{A}$ is an $N \times N$ matrix where N is the number of retrieval levels.

The AK matrix provides three pieces of information (see Maddy and Barnet, 2008, for details): (1) the vertical distribution of information content received from the instrument's radiances, (2) the *verticality*, and (3) an approximation of the instrument's vertical *resolution*; the full-width half maximum (FWHM) of the AK peak is one way to estimate resolution. The vertical distribution of information tells us where the retrieval information content is coming from as a function of pressure. The *verticality*, which is the sum of the ith row in $\mathbf{A}$, tells us how much total information is gathered from the radiances. A verticality near unity indicates the retrieval, for a particular level, comes primarily from the measured radiances, while low verticalities indicate more influence from the a priori.

Figure 1c shows the set of MLS AK's. Notice that all the kernels peak at the correct pressure levels. Note also the verticality (dash-dotted line) is nearly unity at all pressure levels as well. Figure 1d and e show a set of tropical and high latitude AK's from AIRS. The lowest pressure level (highest in altitude) AIRS peaks at (Fig. 1d) is around 260 hPa (there is a peak around 170 hPa, but the verticality for this level is ~0.65, much lower than for higher pressure levels). The MLS verticality indicate that its information content primarily comes from the measured radiances at all levels while AIRS verticality decreases sharply beyond 260 hPa. Although the AIRS verticalities drop off at pressures below 260 hPa, the verticalities still indicate AIRS has some sensitivity to H_2O depending on mixing ratio and local temperature lapse rates; this will be discussed in more detail in Sect. 3.1. A sample extra-tropical sounding shows verticality that peaks around 400 hPa then rapidly drops off at lower pressures (Fig. 1e). As will be shown, this sharp drop in information content occurs for all AIRS H_2O retrievals throughout the tropics and extra-tropics (at higher latitudes the decreases begin further down in the troposphere; see Fig. 1e).

3 Results

3.1 Averaging kernel statistics

One year (2008) of co-located AIRS and MLS profiles is analyzed in a 40 S–40 N latitude band, limited to AIRS profiles with a quality flag of "PGood" (see Level-2 QA and Error Estimation for quality flag details). Figure 2 summarizes the statistical findings. Each row represents a particular retrieval pressure level. In this study pressures between 83 hPa (lower stratosphere) and 407 hPa (free troposphere) are analyzed. Column 1 shows the vertical distribution the AK peaks for the aforementioned retrieval levels; column 2 shows the distribution of verticality, herein termed the *total verticality* (TV); and column 3 shows the verticality but for a narrow set of layers encompassing the retrieval level of interest; herein termed the *local verticality* (LV). This narrow layer spans six atmospheric levels on either side of the retrieval location, totaling 13 levels (out of the 100 possible levels) that go into computing LV (remember that TV is computed summing the AK values for all 100 pressure levels).

From column 1 of Fig. 2 it can be observed that AIRS AK's generally peak at or near the retrieval level up to the 260 hPa level. This suggests that most of the retrieval information content comes from the correct parts of the atmosphere up to 260 hPa. Moving deeper into the UT and transitioning to the tropical tropopause layer (TTL) region (70–150 hPa, Fueglistaler et al., 2009), the kernels generally peak at 260 hPa and at 170 hPa. In fact, from 170 hPa to 83 hPa, the kernel peak distribution does not change much at all, indicating that AIRS has little to no sensitivity to H_2O in this region of the atmosphere. Note that the AK's never peak near the 212 hPa level indicating that AIRS has a "blind spot", i.e. weaker sensitivity in that location of the atmosphere.

Transitioning to column 2 of Fig. 2 one can see that in addition to the AIRS retrievals sensing the expected region in the free troposphere to the lower parts of the UT (260–407 hPa), the retrievals also receive most of the information content from the measured radiances, i.e. TV near unity. From about 212 hPa and upwards the TV drops off rapidly suggesting that AIRS has reduced sensitivity to H_2O in the UTLS. One thing to note is

that even though TV may be near unity, this does not imply strong sensitivity to H_2O for a particular level. The TV provides a cumulative representation of the information content of the retrieval. It does not indicate which vertical layer(s) the information comes from. Column 3 serves to draw out this missing information.

The LV, shown in column 3 of Fig. 2, represents the verticality for a relatively narrow layer around the retrieval level. This parameter serves to extract the fraction of the TV that comes from this narrow band of pressures. AIRS can be considered highly sensitive to H_2O for a particular level when LV is a significant fraction of TV as long as TV (quantified in column 2) is near unity. However, if LV is a small quantity compared to its corresponding TV, this suggest a high degree of correlation between multiple layers far removed from the retrieval level. Note, LV is computed for MLS and the values are a significant fraction of the MLS TV ($\frac{\mathrm{LV}}{\mathrm{TV}} \geq 0.9$).

The mean relative difference of all LV to all TV, $\frac{1}{N}\sum\frac{\mathrm{LV}-\mathrm{TV}}{\mathrm{TV}}$ (for N measurements, reported as a percent), is shown as the first value in each parenthesis (column 3). These percent differences quantify the fraction of the total verticality within in a narrow layer around the retrieval level of interest. LV between 407–314 hPa falls offs by only ∼13%. The 260 hPa level shows first indication of LV falling off abruptly (30%). This, is due in part to the TV distribution being slightly skewed to higher values than at higher pressures. Also, the mean TV at 260 hPa is ∼10% greater than the mean TV for higher pressure levels; the mean LV at 260 hPa is ∼0.8. Above this level the mean LV drops off rapidly, and the distribution of LV shifts quickly to lower values as well, suggesting a loss of sensitivity to H_2O in the TTL region and above.

The second set of values in the parenthesis represent the mean percent change in LV relative to the mean LV at 407 hPa. The average LV from 407 hPa to 260 hPa only falls off by ∼9%, suggesting that AIRS is sensitive to H_2O at these levels. Note that at 314 hPa the LV distribution is broader than its TV counterpart, indicating AIRS is losing some ability to discriminate between levels around this layer and the a priori having some influence on the retrieved profile. Nevertheless, the information content is still very high, giving us confidence in the ability of AIRS to measure H_2O in the lower

parts of the UT in the tropical and extra-tropical atmosphere. The region between 83–212 hPa, which encompasses the TTL, is marked by a mean LV drop from ∼39% to ∼98%, clearly showing that the information content at these retrieval level drops off rapidly. The higher altitude TV distributions suggest that there is some information gleaned from the measured radiances, i.e. non-zero TV, however, this information is mainly obtained from the 170 hPa and 260 hPa levels (see column 1 of Fig. 2) essentially indicating that AIRS is spuriously moving information from lower levels to higher levels where it has little to no sensitivity.

One can argue that AIRS provides high quality H_2O retrievals in the tropics and extra-tropics for pressures as low as ∼260 hPa, or perhaps to lower pressures in moister conditions with discernible vertical thermal gradients. This, however, is not true for higher latitudes. Figure 3 shows the same statistics as shown in Fig. 2 for all latitudes outside the 40 S to 40 N latitude band. Figure 3 reveals that AIRS loses sensitivity starting at around the 314 hPa level. This is seen by the abrupt drop in the mean LV by about 22% relative to the LV at 407 hPa, and by the broadening of the TV and LV distributions starting at the 314 hPa level. This broadening, that also occurs at lower pressures, indicates that retrievals at these level are strongly influenced by the a priori. The UTLS kernel peak distributions also peak at many more levels outside this region of the atmosphere (column 1).

In general, AIRS is sensitive to regions with relatively higher concentrations of H_2O (e.g. the tropical atmosphere) and where there is a thermal lapse rate. However, it is important to determine if the averaging kernels reflect this assumption. Figure 4 shows probability distribution functions (PDF's) of H_2O (columns 1 and 2), temperature lapse rate (dT/dP, column 3) and LV (column 4) at each retrieval level partitioned by various levels at which the AK's peak. Column 1 shows PDF's for the final AIRS retrievals while column 2 shows H_2O distributions of the a priori passed into the AIRS retrieval algorithm (in actuality the a priori in the version 5 dataset are the retrieval profiles after one iteration of the retrieval algorithm). Each curve (in all columns) represents a PDF of values that correspond to where the kernels primarily peak for each retrieval level;

each graph shows a set of three retrieval levels that correspond to the most statistically significant pressure levels shown in column 1 of Fig. 2. For each retrieval level, the red curves show distributions that peak near or at the retrieval level of interest (at 170 hPa the curve is black). We focus on the region where AIRS has weak to strong sensitivity (Fig. 2) to H_2O (170 hPa to 407 hPa).

Comparing column 1 and column 2 in Fig. 4 one finds that the H_2O PDF's noticeably differ. This reflects the high LV (column 4) and TV (column 2 of Fig. 2) values. At most of these levels (pressures greater than 212 hPa) the LV reflects that the majority of the data is not largely governed by the a prior information content. Looking more closely at column 1 the curves corresponding to the retrieval level, or nearest the retrieval level, are more moist than than distributions with peak kernel values differing from the retrieval height (when the AK's peak at the correct pressure level the curves are plotted in solid bold lines). This indicates that AIRS has higher sensitivity to H_2O in more moist atmospheric conditions. The blue and black curves represent distributions of H_2O corresponding to situations when the AK's peak at some layer below or above the retrieval level, respectively. For 170 hPa the red and blue curves are both at higher pressures than the retrieval level because the AIRS AK's never peak at pressures lower than 170 hPa. The LV distributions (column 4 of Fig. 4) follow the H_2O distributions, i.e. moister distributions correspond to higher LV values.

Column 3 shows that the temperature lapse rate distributions closest to or at the retrieval levels, in general, have larger gradients than the distributions at levels at other pressure levels; this is particularly true between 170–314 hPa. This is not surprising as the H_2O IR signature is not only dependent on the concentration of H_2O, but also on the presence of a vertical thermal gradient.

3.2 Merging profiles

The AIRS AK's were shown to have skill in identifying the pressure levels where it can and cannot retrieve H_2O well. The fact that previous intercomparisons confirmed that the AIRS and MLS agree best between 250–260 hPa (Read et al., 2007; Fetzer

et al., 2008), also indicates the AIRS AK's do accurately quantify its sensitivity to H_2O. Since AIRS and MLS both have sensitivity to H_2O and agree best around 260 hPa it is conceivable to merge their profiles with 260 hPa acting as an anchor point between the AIRS and MLS profiles. This requires a method to smoothly transition between the AIRS and MLS profiles and is described below.

In order to merge the profiles the AIRS and MLS AK's are computed on the MLS levels; the AIRS H_2O are also interpolated ($\log(P)$ vs. $\log(H_2O)$) to the MLS levels. This is necessary as the 12 levels per decade for MLS leads to a coarser pressure grid than the AIRS L2 support product levels in the UTLS. This procedure, in effect, redistributes the information content in the 100×100 AIRS AK's matrix onto a 47×47 matrix corresponding to the 47 MLS pressure levels, resulting in two AK matrices, **A** and **M**, that represent the AIRS and MLS AK's, respectively. Furthermore, since the MLS AK's are only available on these levels, the final hybrid pressure grid comprises of MLS pressure levels from the top of the atmosphere down to 261 hPa and AIRS pressure values from 272 hPa down to 1013 hPa.

After computing **A** and **M** the local verticality (LV) is computed from these AK matrices using AK values from the i, $i-1$, and $i+1$ pressure levels, approximating the FWHM of the MLS AK's. Since we are determining which instrument has more sensitivity to H_2O over the same layer of the atmosphere, LV is computed for each instrument over the same range of pressure levels. The AIRS H_2O profiles are kept from 1013 hPa up to 261 hPa (based on the statistics in Fig. 1), and LV is computed from 215 hPa up through the rest of the atmospheric column. All LV serve as weighting coefficients for merging the AIRS and MLS H_2O profiles. This weighting procedure will be discussed in more detail below.

To finally merge the AIRS and MLS profiles a weighted mean between the AIRS and MLS H_2O values is computed, starting from 215 hPa and upwards in altitude, using the

computed LV or weighting coefficients in the following manner:

$$\mathbf{q}_i^{\text{join}} = \frac{\mathbf{q}_i^{\mathbf{A}}\,\text{LV}_i^{\text{A}} + \mathbf{q}_i^{\mathbf{M}}\,\text{LV}_i^{\text{M}}}{\text{LV}_i^{\text{A}} + \text{LV}_i^{\text{M}}}, \tag{3}$$

where $\mathbf{q}_i^{\mathbf{A}}$, $\mathbf{q}_i^{\mathbf{M}}$, and $\mathbf{q}_i^{\text{join}}$ are the H_2O concentrations at the ith retrieval level for AIRS, MLS, and the newly merged profile, respectively. LV_i^{A} and LV_i^{M} denote LV's for AIRS and MLS, respectively. The black dotted line in Fig. 1b is a sample resultant profile from merging the MLS (blue) and AIRS (red) profiles. One observation is that the merged profile has no discontinuities anywhere near the merge region. Furthermore, as will be the case for all merged profiles, it is constrained by the AIRS and MLS H_2O values, i.e.:

$$\mathbf{q}_i^{\mathbf{A}} \le \mathbf{q}_i^{\text{join}} \le \mathbf{q}_i^{\mathbf{M}} \quad \text{or}$$
$$\mathbf{q}_i^{\mathbf{M}} \le \mathbf{q}_i^{\text{join}} \le \mathbf{q}_i^{\mathbf{A}}.$$

Figure 1b demonstrates that the selected co-located profiles can be joined in this manner to create a smooth continuous H_2O profile.

In order to quantify if this technique, at a minimum, produces smooth functions for all merged profiles, the parameter depicted in Fig. 5a–d is computed. The parameter,

$$\text{DQ} = \frac{1}{\delta P}\frac{\delta q}{\mathbf{q}_{i+1}} \tag{4}$$

with $\delta q = \mathbf{q}_i - \mathbf{q}_{i+1}$, represents the percentage change in H_2O between the i and $i+1$ level, scaled by the pressure change δP ($\delta P = P_i - P_{i+1}$) to remove the effect of having a varying pressure grid. This can also be interpreted as a distribution of H_2O lapse rates with respect to pressure, reported as a percent deviation from the $i+1$ retrieval level. DQ is used in order to more clearly identify possible unphysical "kinks" in the profiles. The colors in the distribution (Fig. 5a–c) denote the frequency of occurrence of lapse rates for the entire 2008 data record.

The quantity DQ is shown for the original MLS (Fig. 5a) and AIRS (Fig. 5b) profiles. One observation is the AIRS DQ is smooth throughout the range of the UTLS (the region where AIRS and MLS overlap in sensitivity), while MLS shows a wider variety of lapse rates. Figure 5c shows the PDF's of lapse rates for the merged data. The distributions from the higher pressures become slightly narrower due to the influence of the AIRS H_2O values. However, as we move to lower pressures, the distributions start to mimic the MLS values because LV_i^A is small at these levels; Fig. 5d depicts this more clearly.

At 261 hPa the JOIN (green) and AIRS (red) data are identical because we selected this level as the lowest pressure level that gives full weight to AIRS. The JOIN and MLS curves (blue) already start to converge at 215 hPa. The AIRS and JOIN values at 178 hPa are more similar for a couple reasons: 1) $LV_i^A \sim 0.5$–0.6 at these levels giving AIRS noticeable influence on the mean profile especially for the moist profiles that have greater values of LV, and 2) the AIRS AK's often peak around 170 hPa (Fig. 2 column 1), while never peaking at 212 hPa. This also explains the similarity of the JOIN and MLS distributions at 215 hPa. Although the distribution of DQ_{178} for AIRS might resemble that of the joined profiles, one needs to remember DQ represents a relative percent change in the H_2O lapse rate which only measures the smoothness of the profiles as a whole, providing no qualitative measure of how well mixing ratios compare at any given level (Read et al., 2007; Fetzer et al., 2008).

From 121 to 83 hPa, the DQ distributions for MLS and the merged data look nearly identical. By the time we reach 83 hPa, the JOIN and MLS curves are virtually identical and have no resemblance to the AIRS DQ distribution. From Fig. 2 we see that the LV_i^A distribution at 83 hPa is strongly skewed towards zero while LV_i^M (see Fig. 1c) is near unity at these levels. Note the total number of high quality merged profiles is limited by the number of usable MLS profiles, leading to fewer merged profiles than the number of high quality AIRS profiles noted in Fig. 2.

Even though the profiles are smooth, we also need to determine if the merged profiles preserve what AIRS and/or MLS interprets as the atmospheric state within the

observational uncertainty of AIRS and MLS. Since the merged profiles are constrained by the AIRS and MLS H_2O concentrations and averaging kernels, the merged profiles at a "zeroth" order level cannot deviate far from either instrument's retrievals. However, characterizing the robustness of this dataset requires determining the merged profiles uncertainty in relation to the stated uncertainties of AIRS and MLS. For pressure levels $P \leq 121$ hPa we expect the MLS uncertainties to be the appropriate metric since the AIRS averaging kernels at these upper levels do not contribute much to the merged profile H_2O concentrations since $LV_i^A < 0.25$ and $LV_i^M \sim 1$. However, for larger pressures down to 215 hPa we expect that both the AIRS and MLS uncertainties will be important constraints on the performance of the merged profiles since LV_i^A and LV_i^M are both non-negligible.

There are only a few studies that quantify the accuracy and precision of AIRS. Divakarla et al. (2006) estimated the AIRS accuracy and RMS to be 25% and 40% at 150 hPa and 200 hPa from comparisons with radiosondes launched from 538 stations around the earth using a limited number of stations between the 40 S–40 N band. Tobin et al. (2006) estimated the AIRS RMS error (between 100–266 hPa) from comparisons with radiosonde measurements over the tropical western Pacific to be between 20–25%. Since these values are still not well constrained, because of the limited spatial coverage of the intercomparisons, a fixed value of 25% for both the accuracy and precision is used for all levels in our computation. We do note that these estimates are likely high as the averaging kernels were not available to smooth the radiosonde data to the AIRS resolution. The MLS stated accuracies of 7%, 8%, 12%, 15%, 17%, and 25% for 83 hPa, 100 hPa, 121 hPa, 147 hPa, 178 hPa, and 215 hPa; and the stated precisions of 15%, 10%, 15%, 20%, 20%, and 40% for the same levels are used (Read et al., 2007).

Figure 6 shows the PDF's (in %) of $(\mathbf{q}^{\text{join}} - \mathbf{q}^{\text{AIRS,MLS}})/\mathbf{q}^{\text{join}}$ for the aforementioned levels. Shown in each panel are the root sum square error (RSSE), i.e. $\text{RSSE} = \sqrt{\sigma_{\mathbf{a}}{}^2 + \sigma_{\mathbf{p}}{}^2}$ ($\sigma_{\mathbf{a}}$ and $\sigma_{\mathbf{p}}$ are the accuracy and precision, respectively), for MLS (solid black vertical

lines) and AIRS (dashed-dot vertical lines). The percentage of $\mathbf{q}^{join}$ that fall within the MLS uncertainties (RSSE=17%, 13%, 19%, 25%, 26%, and 40%) or AIRS uncertainties (RSS=35% for all levels) are 99.9%, 99.8%, 94.9%, 84.7%, 96.6%, and 88.7%. For 83 hPa and 100 hPa we expect that most of $\mathbf{q}^{join}$ will fall within the uncertainties since H_2O concentrations at these levels are almost completely influenced by MLS. For the levels below, we still have $\mathbf{q}^{join}$ that fall within the either instruments uncertainty estimates for at least ~85% of the time. Therefore, we can conclude that the newly constructed H_2O profiles do not deviate significantly (more than 1 standard deviation) from the original retrievals within their stated uncertainties. For the values that do fall outside the error estimates, it is noted that they are constrained by either instruments H_2O concentrations, weighted by LV. Thus, even these values do not deviate far from either instruments retrievals.

In order to robustly validate the merged profiles one would need to compare these profiles with a large set of radiosonde measurements that capture a variety of atmospheric conditions. Subsequently, one would need to also apply AK's of both the AIRS and MLS instruments to account for the coarser remote sensing resolution. It is unclear how to apply the AK's for this application because the new profiles represent a weighted mean of AIRS and MLS for $P \leq 215$ hPa. However, even without a detailed intercomparison with in-situ measurements, the merged profiles do not deviate far from the AIRS and MLS soundings within their stated uncertainties for a majority of the profiles.

3.3 Mean H_2O maps

In Sect. 3.2 a combined AIRS/MLS merged profile was constructed. It was shown that the profiles are smooth and do not substantially deviate from the AIRS and MLS soundings within their instrumental uncertainties. Figure 7 shows global maps (July–September, 2008) of H_2O concentrations for 147, 215, 261, and 300 hPa between 40 S–40 N. All maps feature a moist UT due to the convection associated with the Indian monsoon. Also apparent are local maxima over land due to convective uplift

as well. These maps compare well with the maps Fetzer et al. (2008) (their Fig. 3), and further support that our new merged dataset does not change the instrumental interpretation of the atmospheric state.

4 Conclusions

We have quantified the sensitivity of the Atmospheric Infrared Sounder (AIRS) to H_2O in the upper troposphere/lower stratosphere (UTLS). For soundings between 40 S–40 N AIRS can reliably quantify H_2O up to ~260 hPa. At lower pressures AIRS sensitivity rapidly drops in relatively drier conditions and somewhat slowly in more moist conditions. At higher latitudes AIRS starts to lose sensitivity at even higher pressures (around 375 hPa). This is a consequence of increased sensitivity in atmospheres with high concentrations of H_2O and larger vertical thermal gradients. The fact that AIRS has high information content (i.e. high total verticality (TV) and local verticality (LV)) up to 260 hPa corroborates previous results that show AIRS and the Microwave Limb Sounder (MLS) best agree between 250–260 hPa. Thus, this indicates that the AIRS AK's have skill in quantifying its sensitivity to H_2O.

The merged profiles in this study correspond to the nearest AIRS pixel to each MLS point. The method described in this study has also been used to merge the profiles by co-locating the three nearest AIRS pixels (at ~45 km resolution) to each MLS point with ~200 km resolution. This produces a dataset that preserves the native AIRS resolution from the surface up to 261 hPa where H_2O gradients are much stronger than in the TTL. Statistics similar to those shown in Fig. 6 were computed on two pixels adjacent to the nearest neighbor point and yielded very similar results.

Since the AIRS and MLS averaging kernels (AK's) have quantitative skill, the information gleaned from the AIRS and MLS AK's helped to produce the first merged H_2O measurement record that spans the entire troposphere and stratosphere. We have also quantified that the merged profiles do not significantly deviate from the original AIRS and MLS soundings and largely remain within their respective uncertainties. It

should be noted that the method used to construct these profiles cannot be applied for all trace gas retrievals. This procedure is valid for H_2O because its concentration falls off exponentially (e-folding height of ∼2 km) and does not have strong gradients and sign reversals in the UTLS as compared to other gases such as ozone, which sharply increase in the lower stratosphere.

Lastly, we do not suggest this methodology is the optimal method to merge these datasets. A complete treatment of the problem would utilize a joint, simultaneous retrieval with the AIRS and MLS radiances. This problem requires much more research on the practical considerations of a joint instrument retrieval algorithm that accounts for the vastly different instrument sensitivity and sampling characteristics between AIRS and MLS. What we have done is develop a method that takes advantage of the overlapping vertical sensitivity of AIRS and MLS and the typical smoothly varying nature of H_2O in the UTLS. The newly constructed profiles now offer the unprecedented opportunity to explore processes that interact between the troposphere and stratosphere in a self-consistent dataset.

Acknowledgements. C. K. Liang was supported by a NASA Earth and Space Science Fellowship and Northrop Grumman Aerospace Systems fellowship. AIRS and MLS data were obtained through the Goddard Earth Sciences Data and Information Services Center (http://daac.gsfc.nasa.gov/). This work was performed at the Jet Propulsion Laboratory, California Institute of Technology.

References

Aumann, H. H., Chahine, M. T., Gautier, C., Goldberg, M. D., Kalnay, E., McMillin, L. M., Revercomb, H., Rosenkranz, P. W., Smith, W. L., Staelin, D. H., Strow, L. L., and Susskind, J.: AIRS/AMSU/HSB on the aqua mission: design, science objectives, data products, and processing systems., IEEE T. Geosci. Remote, 41, 253–264, 2003. 2835

Divakarla, M. G., Barnet, C. D., Goldberg, M. D., McMillin, L. M., Maddy, E., Wolf, W., Zhou, L., and Liu, X.: Validation of atmospheric infrared sounder temperature and water vapor re-

trievals with matched radiosonde measurements and forecasts, J. Geophys. Res., 111, D09S15, doi:10.1029/2005JD006 116, 2006. 2846

Dunkerton, T.: A two-dimensional model of the quasi-biennial oscillation, J. Atmos. Sci., 42, 1151–1160, 1985. 2834

Fetzer, E. J., Read, W. G., Waliser, D., Kahn, B. H., Tian, B., Vömel, H., Irion, F. W., Su, H., Eldering, A., de la Torre Juarez, M., Jiang, J., and Dang, V.: Comparison of upper tropospheric water vapor observations from the microwave limb sounder and atmospheric infrared sounder, J. Geophys. Res., 113, D22 110, doi:10.1029/2009JD010 000, 2008. 2835, 2836, 2842, 2845, 2848

Fueglistaler, S., Dessler, A. E., Dunkerton, S., Folkins, I., Fu, Q., and Mote, P. W.: Tropical tropopause layer, Rev. Geophys., 47, RG1004, doi:10.1029/2008RG000267, 2009. 2839

Gettelman, A., Randel, W. J., Massie, S. T., Wu, F., Read, W., and Russell, J.: El Niño as a natural experiment for studying the tropical tropopause region, J. Climate, 14, 3375–3392, 2001. 2834

Gettelman, A., Weinstock, E. M., Fetzer, E. J., Irion, F., Eldering, A., Richard, E. C., Rosenlof, K. H., Thompson, T. L., Pittman, J. V., Webster, C. R., and Herman, R. L.: Validation of aqua satellite data in the upper troposphere and lower stratosphere with in situ aircraft instruments, Geophys. Res. Lett., 31, L22 107, 2004. 2835

Gettelman, A., Fetzer, E. J., Eldering, A., and Irion, F.: The global distribution of supersaturation in the upper troposphere from the atmospheric infrared sounder, J. Climate, 19, 6089–6103, 2006. 2835

Hamilton, K.: Mean wind evolution through the quasi-biennial cycle in the tropical lower stratosphere, J. Atmos. Sci., 41, 2113–2125, 1984. 2834

Holton, J. and Gettleman, A.: Horizontal Transport and the dehydration of the stratosphere, Geophys. Res. Lett., 28, 2799–2802, 2001. 2834

Horváth, A. and Soden, B. J.: Lagrangian diagnostics of tropical deep convection and its effect upon upper-tropospheric humidity, J. Climate, 21, 1013–1028, 2007. 2834

Kahn, B. H., Liang, C. K., Eldering, A., Gettelman, A., Yue, Q., and Liou, K. N.: Tropical thin cirrus and relative humidity observed by the Atmospheric Infrared Sounder, Atmos. Chem. Phys., 8, 1501–1518, doi:10.5194/acp-8-1501-2008, 2008. 2835

Kahn, B. H., Gettelman, A., Fetzer, E. J., Eldering, A., and Liang, C. K.: Cloudy and clear sky relative humidity in the upper troposphere observed by the A-train, J. Geophys. Res., 114, D00H02, doi:10.1029/2009JD011 738, 2009. 2835

Kiladis, G. N., Straub, H. K., Reid, G. C., and Gage, K. S.: Aspects of interannual and intraseasonal variability of the tropopause and lower stratosphere, Q. J. Roy. Meteor. Soc., 127, 1961–1983, 2001. 2834

Livesey, N. J., Snyder, W. V., Read, W. G., and Wagner, P. A.: Retrieval algorithms for the EOS microwave limb sounder (MLS), IEEE T. Geosci. Remote, 44, 1144–1155, 2006. 2836

Maddy, E. S. and Barnet, C. D.: Vertical resolution estimates in version 5 of AIRS operational retrievals, IEEE T. Geosci. Remote, 46, 2375–2384, 2008. 2836, 2837, 2838

Read, W. G., Lambert, A., Bacmeister, J., Cofield, R. E., Christensen, L. E., et al.: Aura microwave limb sounder upper tropospheric and lower stratospheric H_2O and relative humidity with respect to ice validation, J. Geophys. Res., 112, D24S35, doi:10.1029/2007JD008 752, 2007. 2835, 2836, 2842, 2845, 2846

Reed, R. J.: The present status of the 26-month oscillation, B. Am. Meteorol. Soc., 46, 374–387, 1965a. 2834

Reed, R. J.: The quasi-biennial oscillation of the atmosphere between 30 and 50 km over Ascension Island, J. Atmos. Sci., 22, 331–333, 1965b. 2834

Rodgers, C. D.: Inverse Methods For Atmospheric Sounding, Theory and Practice, vol. 2 of Series on Atmospheric, Oceanic and Planetary Physics, World Scientific, 2000. 2837

Sherwood, S. C. and Dessler, A. E.: A Model for transport across the tropical tropopause, J. Atmos. Sci., 58, 765–779, 2001. 2834

Sherwood, S. C. and Dessler, A. E.: Convective mixing near the tropical tropopause: insights from seasonal variations, J. Atmos. Sci., 60, 2674–2685, 2003. 2834

Soden, B. J.: The impact of tropical convection and cirrus on upper tropospheric humidity: a Lagrangian analysis of satellite measurements, Geophys. Res. Lett., 31, L20104, doi:10.1029/2004GL020980, 2004. 2834

Soden, B. J., Held, I. M., Colman, R., Shell, K. M., Kiehl, J. T., and Shields, C. A.: Quantifying climate feedbacks using radiative kernels, J. Climate, 21, 3504–3520, 2007. 2835

Solomon, S., Rosenlof, K. H., Portmann, R. W., Daniel, J. S., Davis, S. M., Sanford, T. J., and Plattner, G.-K.: Contributions of stratospheric water vapor to decadal changes in the rate of global warming, Science, 327, 1219–1223, 2010. 2835

Stephens, G. L., Vane, D. G., Boain, R. J., Mace, G. G., Sassen, K., Wang, Z., Illingworth, A. J., O'Connor, E. J., Rossow, W. B., Durden, S. L., Miller, S. D., Austin, R. T., Benedetti, A., Mitrescu, C., and Team, C. S.: The CloudSat mission and the A-train: a new dimension of space-based observations of clouds and precipitation., B. Am. Meteorol. Soc., 83, 1771–

1790, 2002. 2835

Susskind, J., Barnet, C. D., Blaisdell, J., Iredell, L., Keita, F., Kouvaris, L., Molnar, G., and Chahine, M.: Accuracy of geophysical parameters derived from atmospheric infrared sounder/advanced microwave sounding unit as a function of fractional cloud clover, J. Geophys. Res., 111, D09S17, doi:10.1029/2005JD006 272, 2006. 2836

Level-2 QA and Error Estimation: AIRS AMSU HSB Version 5 Level 2 Quality Control and Error Estimation, http://disc.sci.gsfc.nasa.gov/AIRS/documentation/documentation.shtml, 2010. 2839

Tobin, D. C., Revercomb, H. E., Knuteson, R. O., Lesht, B. M., Strow, L. L., Hannon, S. E., Feltz, W. F., Moy, L. A., Fetzer, E. J., and Cress, T. S.: ARM site atmospheric state best estimates for AIRS temperature and water vapor retrieval validation., J. Geophys. Res., 111(18), D09S14, doi:10.1029/2005JD006103, 2006. 2846

Waters, J. W., Froidevaux, L., Harwood, R. S., and Jarnot, R. F.: The earth observing system microwave limb sounder (EOS MLS) on the Aura satellite, IEEE T. Geosci. Remote, 44(5), 1075–1092, 2006. 2835

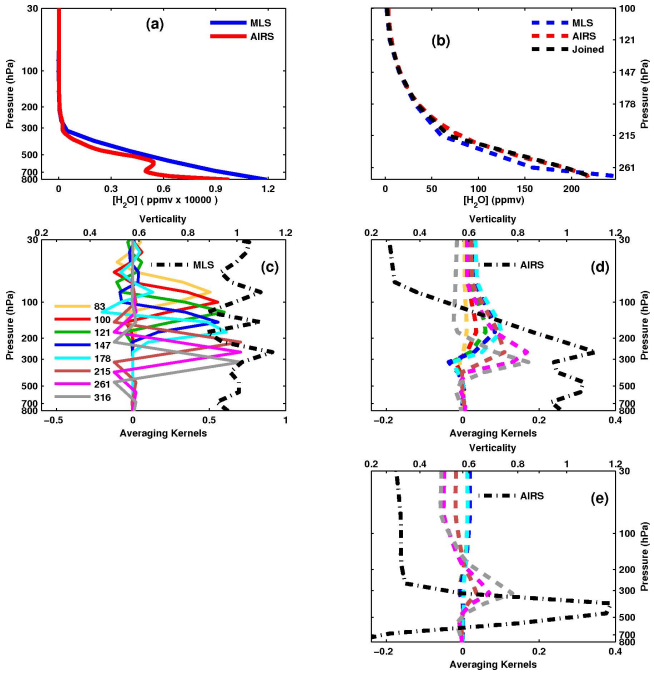

Fig. 1. **(a)** Sample co-located tropical H_2O profiles for AIRS (red) and MLS (blue) at 0.17 N and 176 W, **(b)** the H_2O profile zoomed in at the levels corresponding to the peaks in the averaging kernels in **(c)** for AIRS (red), MLS (blue), and a merged version of the profile (see text for details). Panel **(c)** shows a sample set of tropical averaging kernels from MLS (solid colored lines) for the pressure levels 83, 100, 121, 147, 178, 215, 261, and 316 hPa; dash-dotted black line is the verticality (values at top abscissa). Panel **(d)** same as **(c)** but for AIRS (at 0.17 N and 176 W). Panel **(e)**, same as **(d)**, but at 82 S and 90 W.

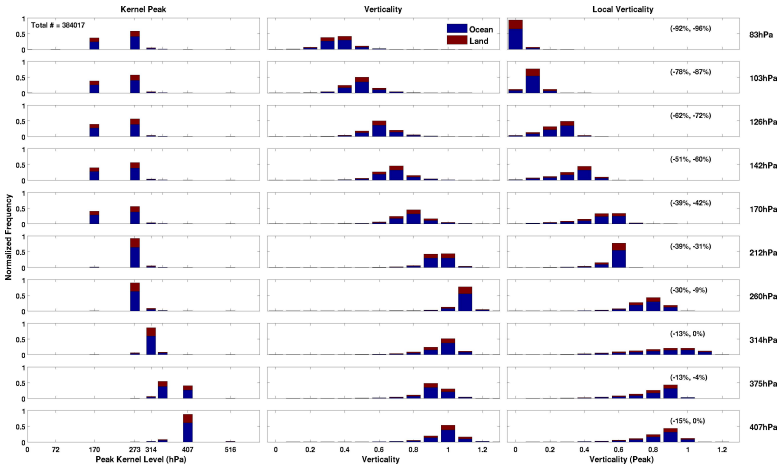

Fig. 2. Distributions of: columun 1) locations of where the averaging kernels peak, column 2) total verticality, and 3) local verticality for each retrieval level at pressures 83, 103, 126, 142, 170, 212, 260, 314, 375, and 407 hPa. Data are for AIRS data only. The total number of profiles is 384,017, so all distributions in column 1 and subsequent columns are normalized to this quantity.

Discussion Paper | Discussion Paper | Discussion Paper | Discussion Paper |

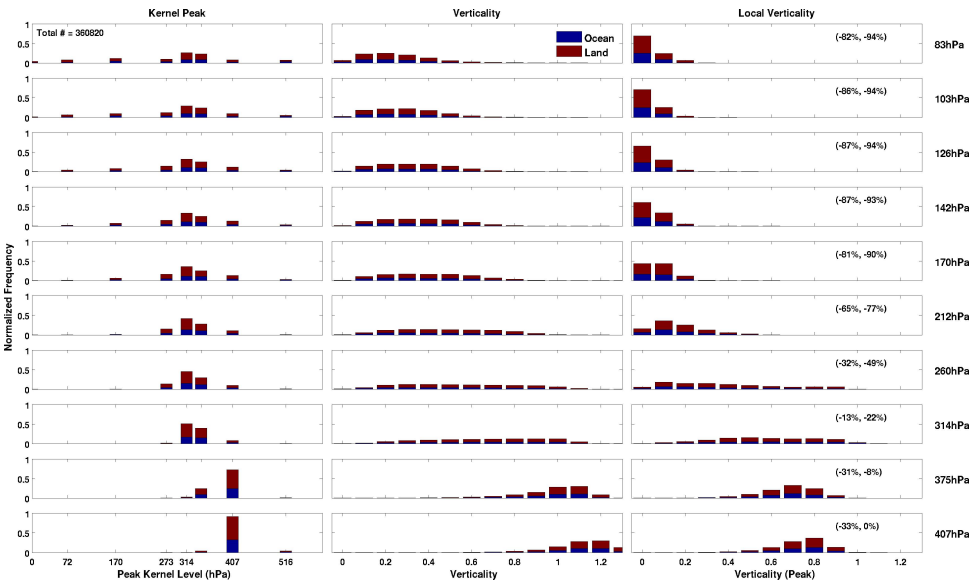

Fig. 3. Same as Fig. 2 but for latitudes polewards of 40 S to 40 N. Total number of profiles is 360 820.

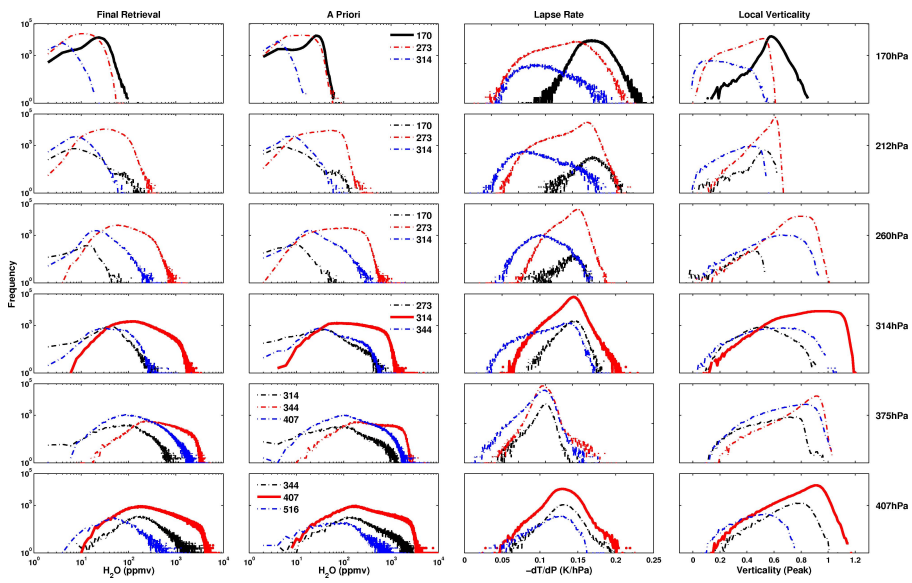

Fig. 4. Distributions of: column 1) H_2O for the final retrieval, column 2) H_2O for the initial guess (a priori), column 3) temperature lapse rate as a function of pressure (note this is $-dT/dP$), and column 4) local verticality for each retrieval level partitioned by the pressure levels where the kernels peak for each retrieval level. Total number of profiles is the same as in Fig. 2. Colors indicate various pressure levels (in hPa) shown in column 2.

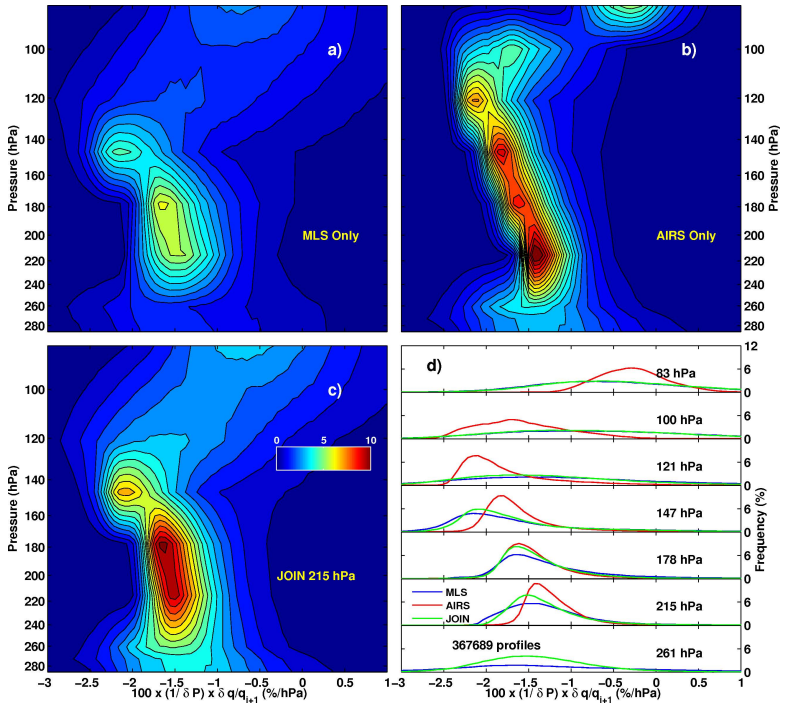

Fig. 5. Joint distribution for the value DQ=$\frac{1}{\delta P}\frac{\delta q}{q_{i+1}}$ (multiplied by 100 to get %) all **(a)** MLS, **(b)** AIRS, and **(c)** joined H_2O profiles. Colorscale shows frequency in %. Panel **(d)** shows the individual PDF's for the joint distributions in **(c)** for pressures of 83, 100, 121, 147, 178 215, and 261 hPa. Frequency units are in % of the total number of profiles shown in the bottom panel in **(d)**. Total number of profiles is 367 689.

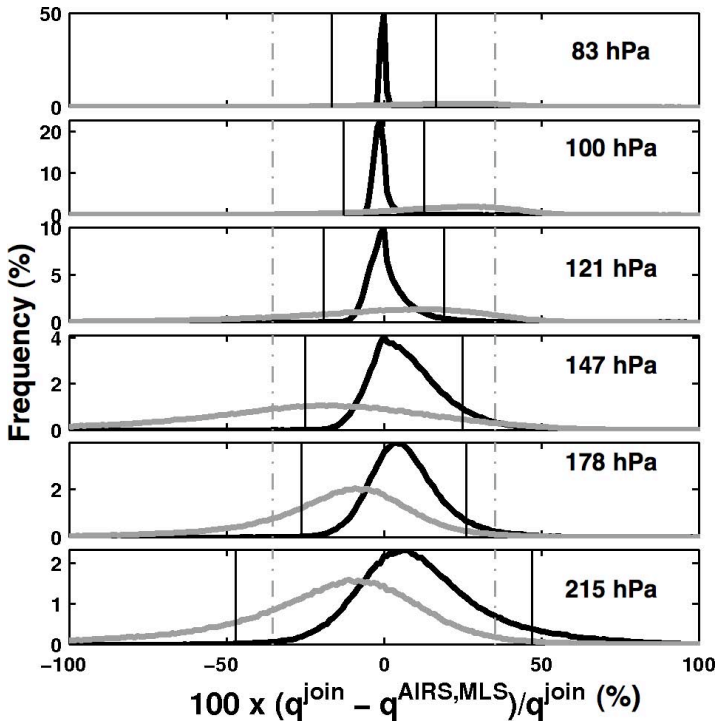

Fig. 6. Percentage difference $(\mathbf{q}^{join}-\mathbf{q}^{MLS})/\mathbf{q}^{join}$ (black curve) and $(\mathbf{q}^{join}-\mathbf{q}^{AIRS})/\mathbf{q}^{join}$ (grey curve) distribution for 83, 100, 121, 147, 178, and 215 hPa (abscissa). Solid black and dashed-dotted grey vertical lines are the root-sum square (RSS) of the accuracy and single profile precision estimates for MLS and AIRS, respectively. Ordinate is frequency reported in percent.

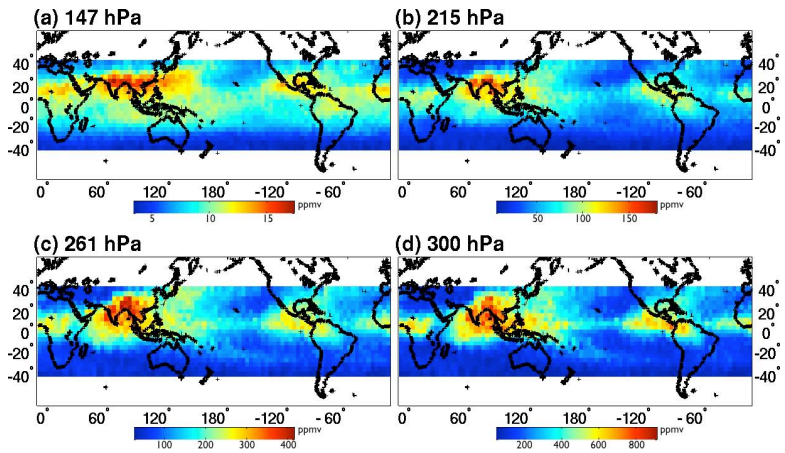

Fig. 7. Mean maps (July 2008–September 2008) of H_2O concentrations binned in 4°×4° grid cells globally between 40 S–40 N for: **(a)** 147, **(b)** 215, **(c)** 261, and **(d)** 300 hPa. Colorscale is in units of ppmv.